Chapter 1

Proton corrections: momentum and efficiency

1.1 Proton momentum corrections

The proton momentum corrections are split in two main contributions. The first corrections, presented in Subsection 1.1.1, are determined by comparing Monte-Carlo generated and reconstructed proton kinematics. The shifts observed in this case is attributed to the energy lost by the proton while propagating in the various detector materials. The determination of the parameters of this correction solely relies on simulations. The second contribution is a data-only based correction, which aims at correcting mis-alignments and inefficiencies of the actual detectors, not accounted for by the simulation. In particular, data-driven corrections are developed for the momenta of the protons in the CD in Subsection 1.1.2.

1.1.1 Monte-Carlo corrections

The Monte-Carlo (MC) momentum corrections for the proton are derived using simulations (BH simulations used in the TCS analysis). The goal of these corrections is to match the momenta of the generated protons with the momenta of the reconstructed protons. These corrections account for the energy lost by the proton while crossing the various detector parts of CLAS12.

The difference between the generated and reconstructed momenta,

$$\Delta P = P_{Gen.} - P_{Rec.}, \tag{1.1}$$

is studied as a function of the polar angle of the proton, θ. The plot in Figure 1.1 shows the difference between the generated and reconstructed proton momenta as a function of θ for protons detected in the FD. The momenta difference shows different behaviors in two distinct regions. Below 27° protons cross little material before being detected and the momentum difference is small (below 20 MeV). Above 27° the material budget between the target and the DCs is larger, especially due to the HTCC and the forward CTOF light-guides. In this region the momentum resolution is degraded and the momentum difference can reach up to 80 MeV.

The MC corrections are derived in three different CLAS12 regions: the two regions in the FD described above and one region in the CD. In each region the momenta difference is parametrized as a function of the reconstructed momentum as shown in Figure 1.2. These corrections are at most of the order of 4% for low-momenta proton (~ 0.45 GeV) in the high-polar angle region of the FD. The corrections are applied to protons in both the simulations and the data.

The corrections functions are second order polynomial in the FD and first order in the CD, defined as:

$$f_{MC}(P) = a_0 + a_1 \cdot P + a_2 \cdot P^2, \tag{1.2}$$

where the coefficient a_i are given in Table 1.1. The corrected momentum then reads:

$$P_{Corr.\ MC} = P_{Uncorr.} + f_{MC}(P). \tag{1.3}$$

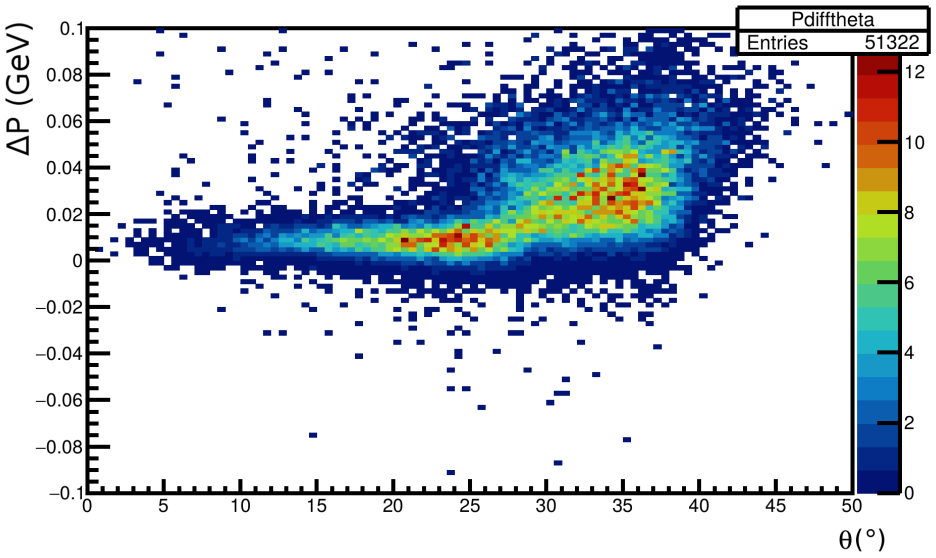

Figure 1.1: Difference between the generated and reconstructed momenta for protons detected in the FD of CLAS12. One can see two distinct regions, below and above $\theta = 27°$.

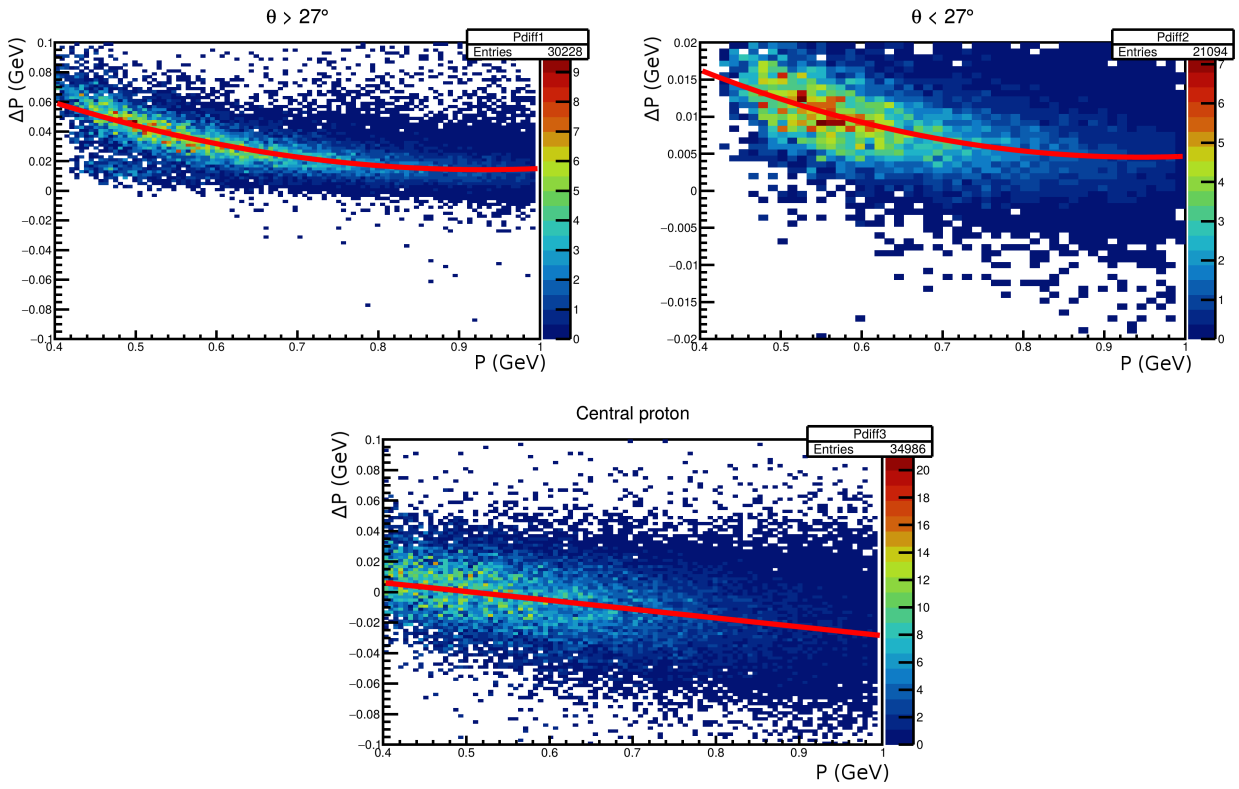

Figure 1.2: Top left: momenta difference (defined in Equation (1.1)) as a function of the reconstructed momentum for polar angles above 27° in the FD. The distribution of the mean of each momentum slice (obtained by a gaussian fit) is fitted with a 2nd order polynomial. The result of this fit is superimposed to the original distribution (red line). Top right: Corresponding figure for protons with polar angles below 27° in the FD. Bottom: Corresponding figure for protons in the CD.

1.1.2 Data-driven momentum corrections

Data-driven momentum corrections for the proton are motivated by the fact that the simulations depict an "ideal" detector, and therefore do not perfectly reproduce the data. Due to the detection

Region	a0	a1	a2
FD ($\theta > 27°$)	0.153319	-0.298968	0.1607
FD ($\theta < 27°$)	0.0398946	-0.0748125	0.0395764
CD	0.0292947	-0.0577956	0

Table 1.1: Values of the coefficients used in the MC-based momentum for proton.

inefficiencies of the CVT, the reconstructed momentum in the CD can be shifted from its actual value. To investigate this issue a method using exclusive two-pion production events was developed. This method relies on the exclusive measurement of the $ep \to e'p'\pi^+\pi^-$ reaction, where the scattered electron and the pions are detected in the FD. The kinematics of the scattered proton can then be studied in two different ways. In one case the proton can be detected by CLAS12, in the other case its kinematics can be inferred by calculating the missing 4-momentum of X in the $ep \to e'\pi^+\pi^- X$ reaction.

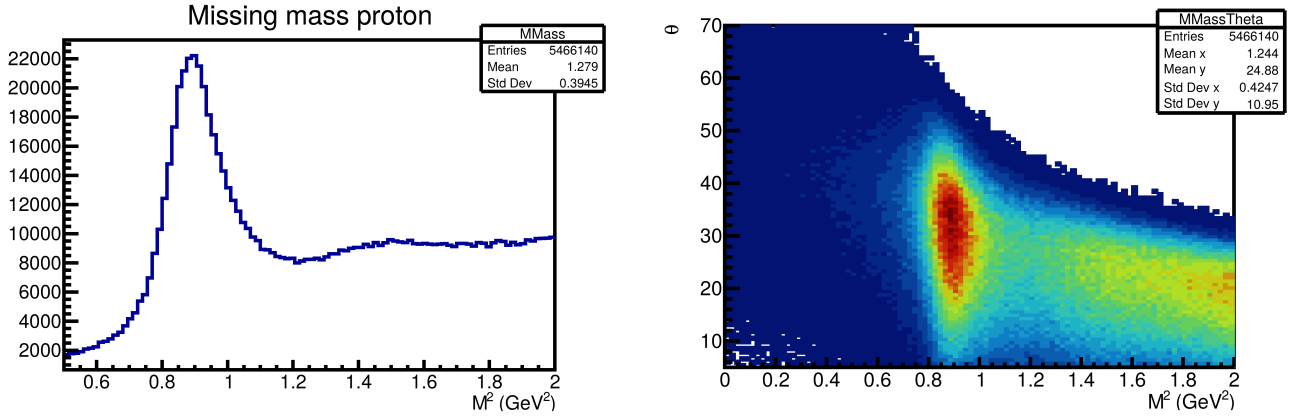

(a) (b)

Figure 1.3: (a) Squared missing mass of the $ep \to e'\pi^+\pi^- X$ reaction. One can see a clear peak at the proton mass and a higher-mass continuum. (b) Missing polar angle as a function of the squared missing mass for the same reaction. Once can see that the high-polar-angle region, corresponding to topologies where the missing proton goes in the CD, is free of high-mass background.

The missing mass spectrum obtained from the latter analysis is shown in Figure 1.3. One can see that the missing mass shows a clear peak at the proton mass. Furthermore, looking at the dependence of the missing mass as a function of the missing polar angle in Figure 1.3b, one can see that at high polar angles (above 35°) the high-mass component is suppressed and the missing mass spectrum has a contribution only from the scattered proton. This allows to compare directly the kinematics of the missing proton to the kinematics of the detected proton.

Figure 1.4 shows the momentum difference:

$$\Delta P = P_{Rec.} - P_{Missing.} \tag{1.4}$$

as a function of the detected polar angles (Figure 1.4a) and the detected momenta (Figure 1.4b). No large dependencies are seen. The momentum resolution defined as:

$$\frac{\Delta P}{P} = \frac{P_{Rec.} - P_{Missing.}}{P_{Rec.}} \tag{1.5}$$

is also plotted as a function of the local azymuthal angle in the last layer of the CVT, ϕ_{CVT}, as shown in Figure 1.5.

Each subplot corresponds to one of the three CVT regions. The azymuthal coordinate of the last layer of the CVT is used for this correction (layer ID 12 in the CLAS12 reconstruction nomenclature).

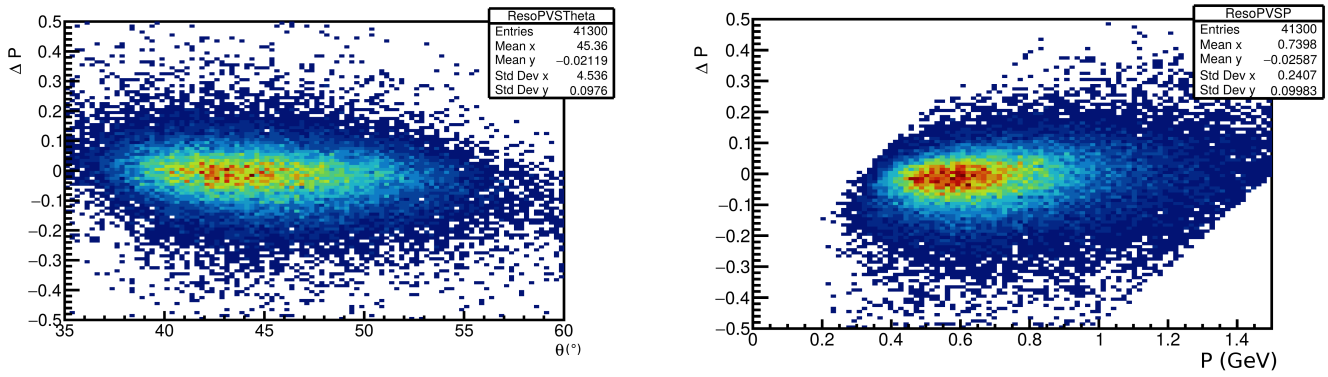

(a) (b)

Figure 1.4: (a) Data-driven momentum difference as a function of the polar angle for protons in the CD. (b) Momentum difference as a function of the momentum.

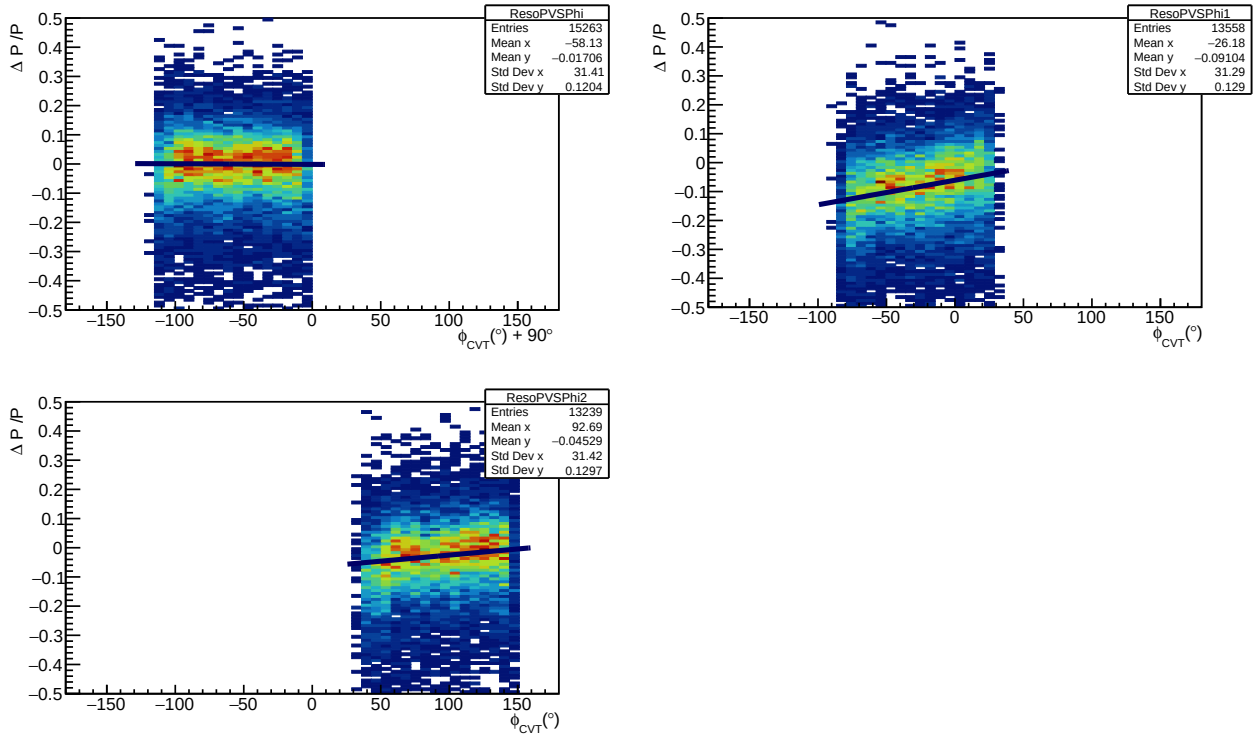

Figure 1.5: Momentum resolution as a function of the local azymuthal angle for protons in the CD, for the three regions of the CVT. The superimposed black line is the correction function for each region.

The distribution of the gaussian means of each ϕ_{CVT} slices is fitted with a linear function, for each subplot. The obtained coefficients are detailed in Table 1.2, where the functions can be written:

$$f_{DATA}(\phi_{CVT}) = c_0 + c_1 \cdot \phi_{CVT}. \tag{1.6}$$

It has to be noted that for the range $-210 < \phi_{CVT} < -90°$ a 90° shit is used for the angle to be in the $[-180°, 180°]$ range. The coefficient given in Table 1.2 are given after this translation. The resulting corrections are applied to the proton momenta in the data. The corrected momentum reads:

$$P_{Corr.\ DATA} = P_{Uncorr.} \cdot (1 - f_{DATA}(\phi_{CVT})). \tag{1.7}$$

The corrections range from almost zero for protons in the region $-210° < \phi_{CVT} < -90°$ to up to

14% at the lower edge of the $-90° < \phi_{CVT} < 30°$ region. These corrections are performed after the MC corrections presented in the previous subsection.

ϕ_{CVT} range	c0	c1
$-120° < \phi_{CVT} + 90° < 0°$	-0.00146068	-2.13735e-05
$-90° < \phi_{CVT} < 30°$	-0.0608671	0.000849025
$30° < \phi_{CVT} < 150°$	-0.0670748	0.000419003

Table 1.2: Values of the coefficients used in the data based momentum for proton in the CD.

1.2 Proton efficiency correction

In order to take into account the differences in the proton detection efficiency between real data and simulations, a proton efficiency correction to the GEMC simulation is implemented. This correction is derived using the same data sample as for the proton momentum corrections discussed in Subsection 1.1.2. The $ep \to e(p')\rho \to e(p')\pi^+\pi^-$ reaction is selected by applying a cut on the invariant mass of the two pions, 0.6 GeV $< M_{\pi^+\pi^-} <$ 1 GeV. This cut allow to simulate the reaction easily. The same reaction is generated using the *genev* event generator and passed through the GEMC and the CLAS12 reconstruction softwares. The kinematics of the missing proton are assumed to be well reconstructed and are used to derive the correction. The MC and data driven corrections described in Section 1.1 are applied prior to the computation of this correction. The proton efficiency is measured for data and simulations as:

$$Eff^{\text{Data/Simu.}}(\Omega_{Mis.}) = \frac{N_{Rec.}^{\text{Data/Simu.}}(\Omega_{Mis.})}{N_{Mis.}^{\text{Data/Simu.}}(\Omega_{Mis.})}, \tag{1.8}$$

where $N_{Mis.}^{\text{Data/Simu.}}(\Omega_{Mis.})$ is the number of events with a missing proton in the kinematic bin $\Omega_{Mis.} = P_{Mis.}; \theta_{Mis.}; \phi_{Mis.})$, $N_{Rec.}^{\text{Data/Simu.}}(\Omega_{Mis.})$ is the corresponding number of events with a detected proton. The proton efficiency correction is then encoded in the ratio:

$$Eff_{Corr} = \frac{Eff^{\text{Data}}}{Eff^{\text{Simu.}}}. \tag{1.9}$$

The correction is computed in the CD and in the FD independently, using similar procedures described in the next two subsections.

1.2.1 Efficiency correction in the central detector

As shown in Figure 1.3b, there is very little background under the missing-proton mass peak in the high-polar-angle region. The number of events with a missing proton or a detected proton is then given by the number of events in each bin. The integrated efficiencies as a function of the momentum, the polar and the azimuthal angles of the missing proton are shown in Figure 1.6. The efficiency calculated in the simulations case is higher than for the data. The efficiency correction is calculated as a function of the three variables, with 2 bins in θ (from 37° to 45° and from 45° to 65°), 4 bins in momentum (spanning the 0.4 to 1.5 GeV range evenly) and 18 bins in ϕ (from $-180°$ to 180°, 20° bins). The limits of the binning are driven by the variation of the correction as a function of each variable. Figure 1.7 shows the value of the corrections. It ranges from 60% to 160%, but it is most of the time around 70% to 80%.

1.2.2 Efficiency correction in the forward detector

The proton efficiency is also derived for FD protons. Unlike in the case of the CD, where there is no background under the proton peak, there is a large high-mass background in the missing mass spectrum for protons at polar angles below 37°. In this region the number of events with a missing or reconstructed proton is calculated by fitting the missing proton peak with a gaussian plus a linear

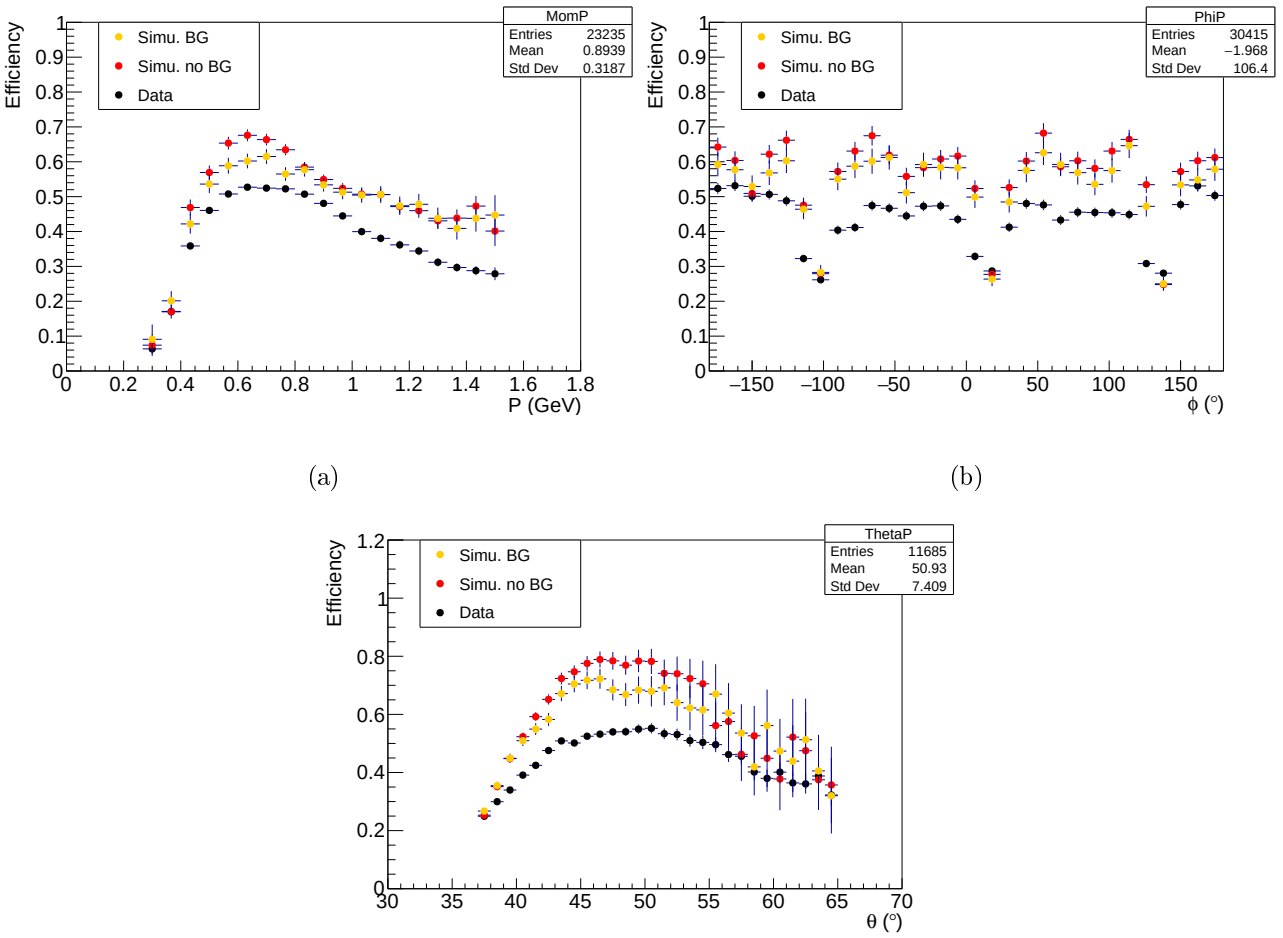

Figure 1.6: Proton efficiency in the CD, as a function of (a) the momentum, (b) the azimuthal angle and (c) the polar angle of the missing proton; for simulations without BG merging in red, with BG merging in yellow and data in black.

background as shown in Figure 1.8. The integral of the gaussian defines the number of events. The fit on the missing mass peak is done in both the missing-proton case and the reconstructed-proton case. In the case of the reconstructed proton, only the events with a reconstructed proton are kept in the missing mass spectrum fit.

Figure 1.9 shows the efficiency as a function of the momentum, the azymuthal and the polar angles of the missing proton. As the ratios between simulations and data efficiencies are fairly constant in θ and ϕ, a single differential correction in momentum is applied according to the efficiencies shown in Figure 1.9a. The correction values are given in Table 1.3. Not that the momentum bin $[0.3, 0.42]$ is assigned the same correction factor as the next bin as the number of data points is too low to allow correct extraction of the efficiency. This change has no effect on the TCS analysis, as most protons have momenta above 0.4 GeV in the CD. This correction factor is at most 0.6, but most of the time close to 1.

Momentum (GeV)	0.3	0.42	0.54	0.66	0.78	0.9	1.02	1.14	1.26	1.38
Eff_{Corr}	0.665*	0.665	0.839	0.957	0.957	1.01	0.963	0.944	0.937	0.916

Table 1.3: Values of the efficiency correction in the FD as a function of the proton momentum.

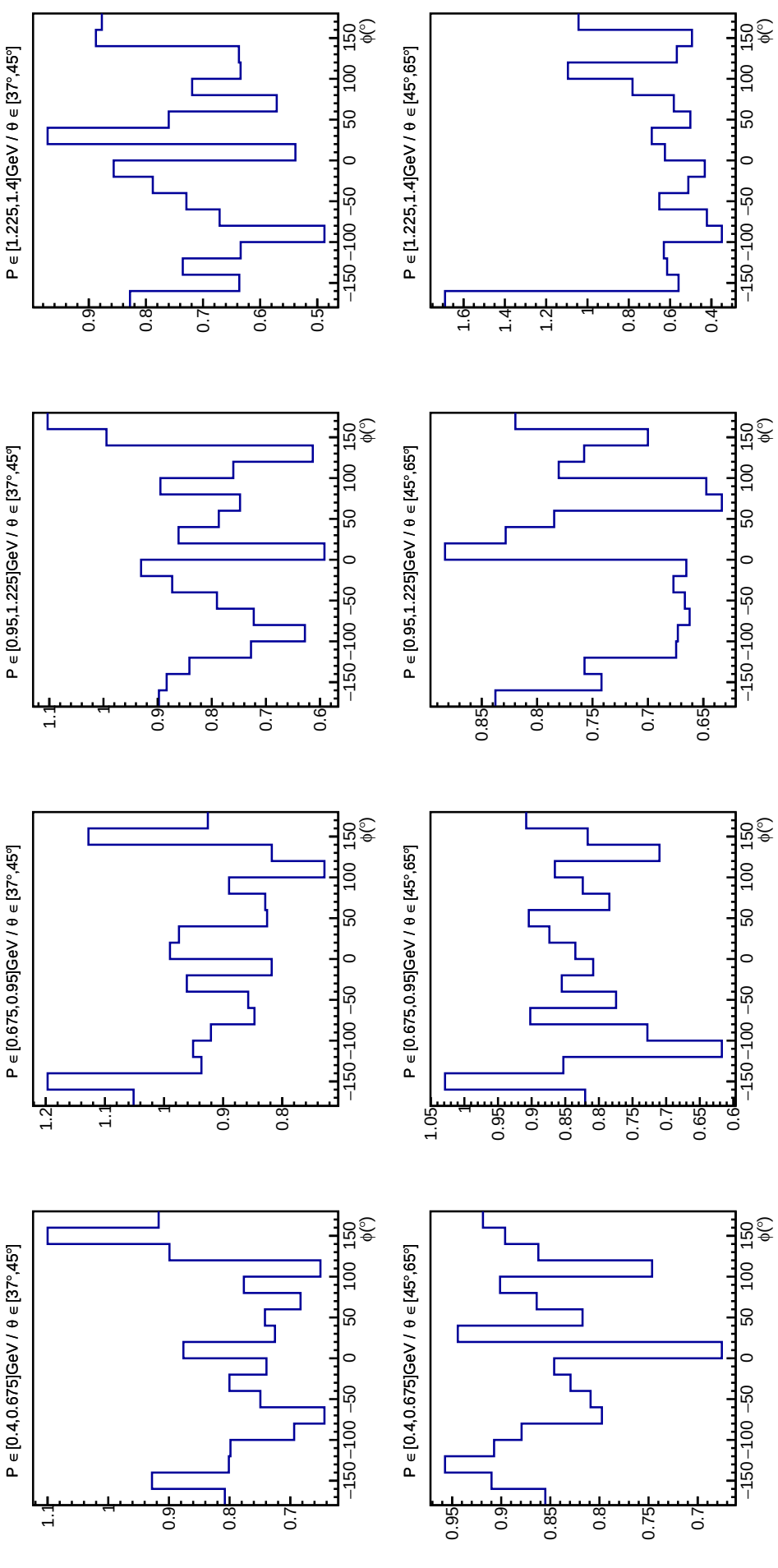

Figure 1.7: Efficiency correction in the CD for two bins in polar angle θ and 4 momenta bins. The correction is given as a function of azymuthal angle of the proton ϕ.

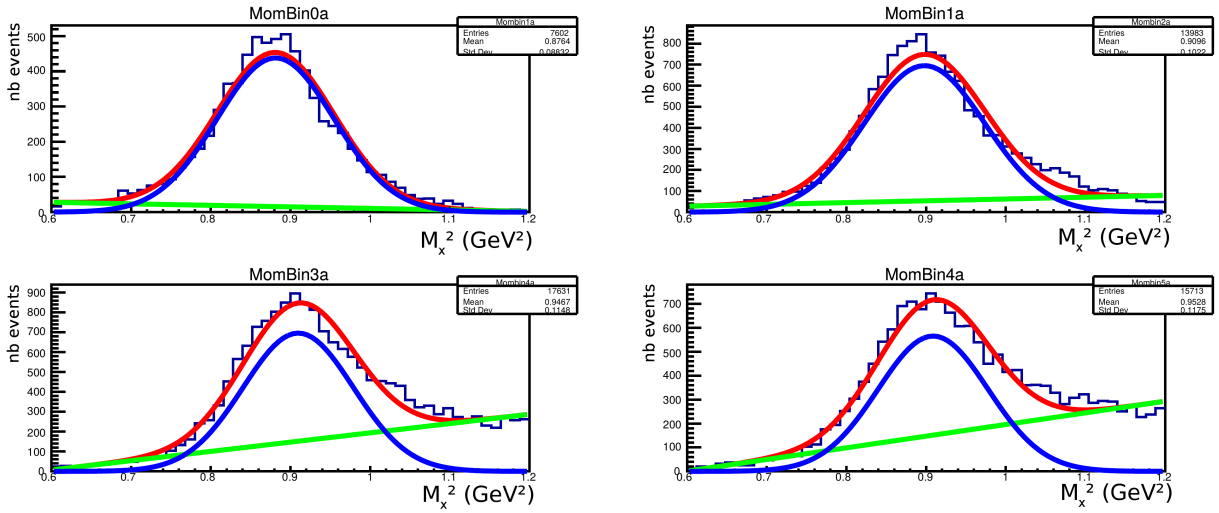

Figure 1.8: Examples of fits performed for the proton efficiency analysis in the FD. The missing mass peak is fitted with a gaussian and a linear background.

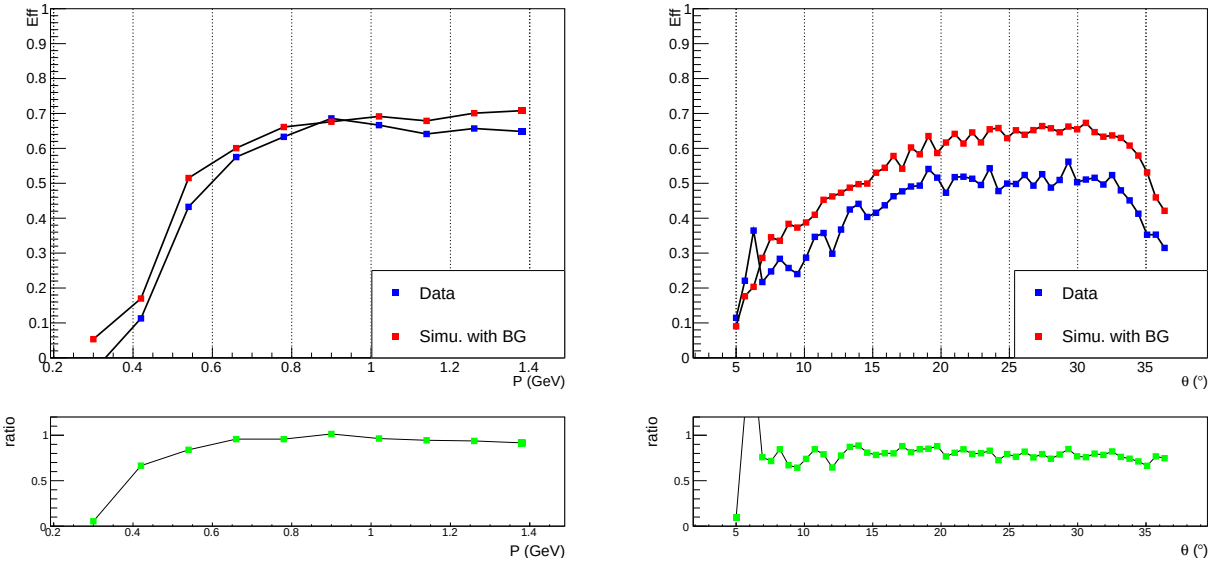

(a) (b)

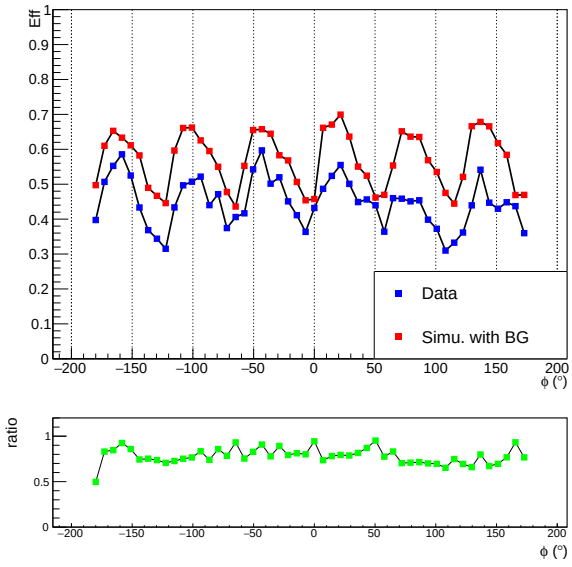

(c)

Figure 1.9: Proton efficiency in the FD, as a function of (a) the momentum, (b) the azimuthal angle and (c) the polar angle of the missing proton; for simulations in red and data in blue.